

PAPER • OPEN ACCESS

Magnetoelastic properties in polycrystalline Fe-Pd based ferromagnetic shape memory alloys

To cite this article: M Sofronie *et al* 2019 *IOP Conf. Ser.: Mater. Sci. Eng.* **485** 012026

View the [article online](#) for updates and enhancements.



IOP | ebooks™

Bringing you innovative digital publishing with leading voices to create your essential collection of books in STEM research.

Start exploring the collection - download the first chapter of every title for free.

Magnetoelastic properties in polycrystalline Fe-Pd based ferromagnetic shape memory alloys

M Sofronie¹, B Popescu¹, AD Crisan¹, AR Lupu^{2,3}, F Tolea¹, M Valeanu¹

¹National Institute of Materials Physics, POB MG-7, 77125 Bucharest-Magurele, Romania

²Victor Babes National Institute of Pathology, Bucharest, Romania

³“Cantacuzino” National Medico – Military Institute for Research and Development, Bucharest, Romania

felicia.tolea@infim.ro

Abstract. Two series of Mn substituted Fe-Pd ferromagnetic shape memory ribbons were studied by X-ray diffraction, calorimetric and thermo-induced strain measurements. Linking the structural, magnetic and thermal expansion analysis on pristine ribbons and those subjected to different subsequent thermal treatments, highlights the role of substitution and of heat treatment of the martensitic transformation (MT). The melt-spinning technique removes the precipitation of undesirable b.c.t. irreversible phase and the addition of Mn, as a third alloying element, promotes the stabilization of the f.c.t. martensite. The linear thermal expansion measurements with and without static magnetic field provide information on the easy magnetization axis in the martensitic structure. Preliminary *in vitro* cytotoxicity tests generally indicate no toxicity or a tendency towards cell proliferation induced by the tested materials.

1. Introduction

Specific to the shape memory alloys (SMA) is the martensitic transformation (MT), a thermo-elastic, reversible structural phase transition between a high symmetry phase (austenite) and a lower one (martensite). On cooling, the high temperature austenite phase undergoes a diffusionless transformation in which atoms shift cooperatively reducing the symmetry and forming the low temperature martensite phase. Ferromagnetic SMA (FSMA) are materials with the MT temperature lower than magnetic order-disorder transition temperatures. The Fe-Pd based ferromagnetic shape memory alloys are promising materials for applications, due to better mechanical properties and a higher magnetic order-disorder transition temperature (~760 K) than Ni-Mn-Ga FSMA. Moreover, the biocompatibility is a significant benefit of Fe-Pd (30 at. %) compared to Ni₂MnGa based Heusler alloy allowing to use this material for biomedical applications, such as stents or pumps [1]. In this system was found that MT is characterized by various possible martensite phases with different degrees of distortions: face-centered tetragonal (f.c.t.) and body-centered tetragonal (b.c.t.). By cooling, a thermo-elastic, reversible transformation from face-centered cubic (f.c.c.) austenite to f.c.t. martensite takes place. When the cooling process continues the tetragonal distortion is enhanced until a new irreversible transformation (IMT) f.c.t.-b.c.t. may be evidenced. The martensitic transformation (MT) from f.c.c. to f.c.t. in disordered Fe-Pd alloys is observed in a narrow composition range, between 29 and 32 at. % Pd [2]. In order to avoid the formation of the undesirable b.c.t. martensite, so to stabilize the f.c.t. martensite, as well as to manipulate the transformation temperatures, the addition of a third alloying element became a challenge. The literature reports a significant increase of transformation temperature (333 K) and a decrease of the non-reversible



transformation temperature for Fe-Pd-Mn ternary bulk system [3]. Rapid solidification, by using a melt-spinning technique, is an effective processing route to obtain ribbons with a non-equilibrium structure, in which the high temperature f.c.c. structure can be frozen as single phase [4]. The present paper emphasizes the influence of Mn addition and thermal treatments in Fe₆₉Pd₃₀Mn₁ and Fe₆₇Pd₃₀Mn₃ melt-spun ribbons on the MT evolution, magneto-elastic properties and biocompatibility, from the perspective of using these materials in applications.

2. Experimental

Alloy ingots of Fe₆₉Pd₃₀Mn₁ and Fe₆₇Pd₃₀Mn₃ were prepared under Ar protective atmosphere, by arc-melting of high purity elements and the procedure was repeated several times in order to ensure homogeneity. The procedure was following by melt-spun into ribbons using melt-spinning technique (3 mm wideness, 10-20 mm lengthiness and 25-30 μm thickness). The pristine ribbons (denoted PMn1 and PMn3) were thermal treated in vacuum quartz ampoules at 950°C for different duration, the samples being denoted ST (short time - 10min at 950°C) and LT (long time-30min at 950°C). Each thermal treatment (TT) was followed by a direct quenching of the sample in iced water. The structural investigations were done by X-ray diffraction (XRD) using a Bruker D8 Advantage diffractometer in the Bragg–Brentano geometry, with Cu K α radiation, at room temperature (RT). The phase transformation temperatures were determined by using a differential scanning calorimeter (DSC) model 204 F1 Phoenix (Netzsch), with a scanning rate of 10 K/min. The chemical composition and the surface morphology of the ribbons were examined by Energy Dispersive X-Ray Spectroscopy (EDX) and Scanning Electron Microscopy (SEM) in a Zeiss Evo 50 XVP microscope. Magnetic measurements were performed by MPMS-SQUID-QD magnetometer in RSO mode, with magnetic field along ribbon direction. The linear thermal expansion (LTE) measurements have been realized by means of two strain gauges, one was glued along the ribbon length and the other serving as reference. The “Vishay Micro-Measurements Model P3 strain indicator and recorder” and the magnetic platform Cryogenic Ltd. were used for fulfilling these determinations. In-plane strains, with the field applied parallel to the ribbon plane were record as a function of temperature. Osteoblast-like cells (MG63) were seeded in 24-well culture plates, in volumes of 1 ml of Dulbecco's Modified Eagle Medium/Nutrient Mixture F-12 (DMEM-F12) complete culture medium (10% fetal bovine serum-FBS), 1% L-glutamine and 1% antibiotics), at a density of 10⁵ cells/cm². After cell adherence and growth (24h), the culture medium was discarded and replaced with fresh medium (1 ml/well) containing floating ferromagnetic ribbons with total surface area of 10, 10/2 and 10/4 mm² respectively. The cells were treated for 24h. Following treatment, the culture medium was removed and replaced with MTT [3-(4,5-Dimethylthiazol-2-yl)-2,5 diphenyltetrazolium-bromide] solution (300 μl /well of 1 mg/ml MTT in phosphate buffered saline (PBS). After 2 hours of incubation, the MTT solution was discarded and 300 μl of dimethyl sulfoxide (DMSO) were added to each well in order to dissolve the produced formazan crystals. The absorbance of the formazan solution was determined at 540 nm with a Thermo Multiskan EX spectrophotometer. Cell viability was quantified and expressed as percent versus control.

3. Results and discussions

DSC scans have been performed in wide temperature range, between 90 and 400 K and it is important to note that MT was evidenced, without IMT for all investigated alloys, as a result of the melt spinning technique. Figure.1 shows DSC records during the cooling/heating sequences which have allowed highlighting MT and identifying its characteristic parameters: martensite start (Ms) and finish (Mf), austenite start (As) and finish, (Af) and the transformation enthalpy (H), calculated as average between the direct and reverse transformation enthalpy. DSC results reveal sharp peaks, the transformation enthalpy is enhanced and Ms drastically increase (~ 40 K) with increasing of Mn substitution [5]. The martensite start temperature (Ms) and the transformation enthalpy (associated with the DSC peak area) values are depicted in Figure.2. The structural transformation on the PM3 sample could not be evidenced by this method probably due to its low enthalpy. Can be seen a surprisingly lower MT temperature for

this sample, determined by thermo-magnetic measurements (marked with dashed line). By reaching the atomic order after the thermal treatments, the effect of Mn substitution is to slightly enhanced of the MT temperatures (~ 5 K) for Mn 1 samples and drastically increasing (~ 60 K) for Mn3 samples.

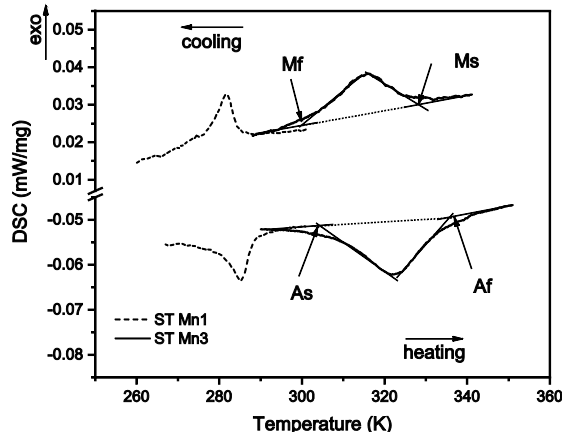


Figure.1. DSC scans after cooling/heating sequence for ST Mn1 and ST Mn3.

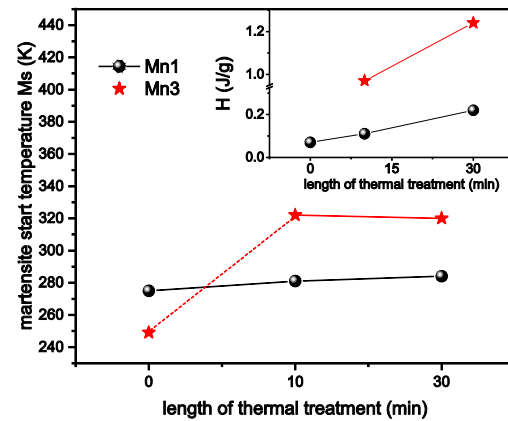


Figure.2. Ms for Mn1 and Mn3 samples (dashed line indicates Ms for P Mn3, determined by thermo-magnetic measurements); Inset: the transformation enthalpy (H).

The transformation enthalpy has a monotonous increase with TTs for Mn1 samples. It has to be noticed the rise of the transformation enthalpy, up to 1.24 J/g, (for LT Mn3), close to that registered in Fe-Pd singlecrystal (30at.% Pd), but 2.5 times higher than one for polycrystalline alloys [2]. The X-ray diffraction patterns (not shown) at room temperature indicate that pristine samples (P Mn1 and P Mn3) exhibit a single highly textured f.c.c. phase, the high temperature stable phase retained in the ribbons due to the rapid cooling, specific for the melt spinning technique. The TTs at high temperature (950°C) induced the f.c.c. microstructure ordering and elimination of the quenched-in stress tensions arising from preparation technique for Mn1 samples. A mixture of f.c.c./f.c.t. phases and rather small content of another phase rich in Pd and Mn (@) was found for TTs Mn3 samples. The SEM images (Figure.3. a-b) indicate small grains and typical twin variant band morphology characteristic to the martensitic phase for Mn3 samples. In addition, the presence of precipitates can be distinguish in the composite matrix, small ($0.5\text{-}1\mu\text{m}$) and rather numerous, which are mainly located at the grain boundaries.

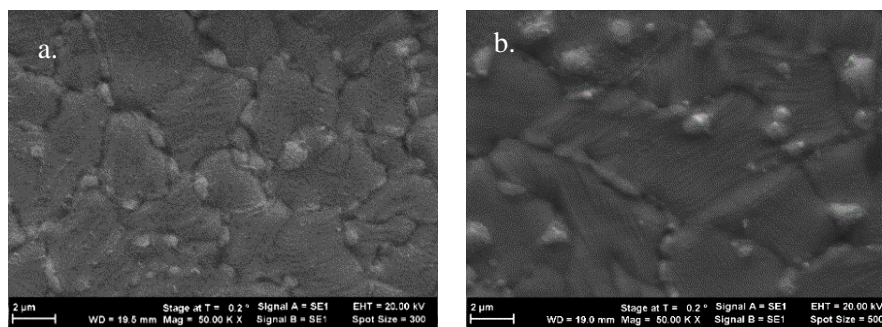


Figure.3. SEM images on ST Mn3 (a) and LT Mn3 (b) surface

The presence of precipitates is the results of the particularly low solubility of Mn in the Fe-Pd system [3]. EDX analysis indicates a decreasing of Pd content in the ST Mn3 and LT Mn3 matrix, supported by the existence of precipitates, which have the chemical compositions close to $\text{Fe}_5\text{Pd}_6\text{Mn}_2$. For Fe-Pd shape memory alloys, a decrease in the Pd content results in an increase of the MT temperatures [6], in agreement with calorimetric results (Figure.2.).

The thermo-magnetic measurements performed at higher temperature (above to 300 K) show the influence of the matrix composition changes on the order-disorder magnetic transition for ST Mn3 and LT Mn3 samples (Figure.4). On the heating curve, the magnetization variation in 300-400 K temperature range is the results of the magneto-crystalline anisotropy change when the structure recovered the austenitic state, after reversible MT. In addition, the abrupt decreases of the magnetization curve observed in 500-600K temperature range, indicates the magnetic order-disorder transition (T_C - Curie temperature). This temperature was determined by derivate of magnetization versus temperature (Inset Figure.4.). During the thermomagnetic measurements, the temperature is increased and then lowered slowly, a process that induces the decomposition of the metastable f.c.c. phase in $L1_0$ -f.c.t. phase and a Fe-rich phase with b.c.c. structure. For ST Mn3 sample the decomposition of the f.c.c. phase is not complete; so, on the cooling branch besides to the magnetization jump at 770K, the Curie temperature for the $L1_0$ phase, a small amount of the austenite with f.c.c. structure having $T_C = 615$ K may be evidenced.

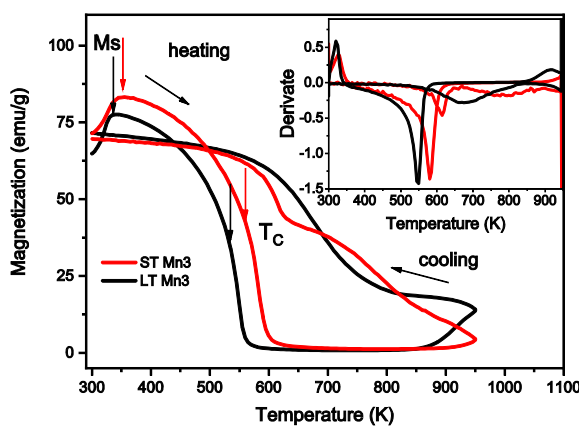


Figure.4. Low field thermo-magnetic measurements (100 Oe) at high temperatures (above to 300 K) of ST Mn3 and LT Mn3 ribbons (inset: Derivate of magnetization versus temperature)

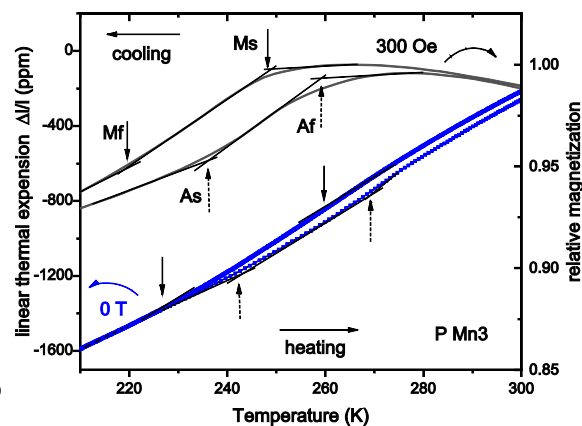


Figure.5. LTE curve during ZFC (zero field cooling) process versus relative magnetization (300 Oe) for ST Mn3 and LT Mn3 samples. The arrows indicate M_s , M_f (solid line) and A_s , A_f (dash line) temperatures

The LT Mn3 sample has a complete decomposition of f.c.c. phase in the stable $L1_0$ phase ($T_C = 680$ K) and a second Fe-rich one with $T_C > 900$ K on cooling branch of magnetization curve and the absence of any other phases. This evolution of thermo-magnetic curves is strongly influence by the process of nucleation and subsequent growth of the precipitates that are influence by the thermal treatment duration. Therefore, increasing the length to 30 min induces a homogenization of multi-phase structure and a decrease of T_C , with reduction of Fe concentration in the sample matrix.

The linear thermal expansion (LTE) results provide information about the relative length-change ($\Delta l/l$) of samples in cooling/heating sequence, with and without applied magnetic field. The change in length is proportional with temperature for a solid material and can be expressed as $\Delta l/l_i = \alpha \Delta T$, ($\Delta l = l_f - l_i$ and $\Delta T = T_f - T_i$) where l_i and l_f represent, the initial and final lengths with the temperature change from T_i to T_f and α is the coefficient of LTE. First, the LTE curves were measured by cooling and heating between 320 and 200 K without magnetic field followed by the same cooling/heating sequence with magnetic field (1T) applied in austenitic phase, parallel to the ribbons length. On cooling and passing through the MT in ZFC (zero field cooling) mode, the ribbons undergo a continuous contraction as a result of the tendency of the variants to accommodate the strain, without preferred direction of growth, in order to minimize the elastic energy and maintain the shape of the ribbons [7]. It's important to notice that, the ZFC curve shows the spontaneous contraction and a weak thermal hysteresis characteristic to MT in 225-270 K temperature range for P Mn3. Therefore, the MT temperatures were estimate, with values in close agreement with those obtained by the thermomagnetic measurements at low magnetic field (300 Oe) (Figure.5). A slightly discrepancy between these temperatures (~ 10 K) obtained from thermal expansion and thermomagnetic data arises from instrumental error, especially for the

thermomagnetic ones (it is impossible to place the thermocouple on the sample surface). Thus, the linear thermal expansion measurements in ZFC mode represent a powerful tool to evidence MT characteristic temperatures in SMA. The MT has been identified by LTE measurements (Figure.6. and Figure.7.) and the values are in close agreement with those obtained by calorimetric measurements (Figure.2.). The arrows indicate M_s (solid line) and M_f (dash line) temperatures. Due to the high temperature limitation of the LTE measurement system (320K), the martensite start (M_s) temperature for ST Mn3 and LT Mn3 samples cannot be detected (Figure.7.).

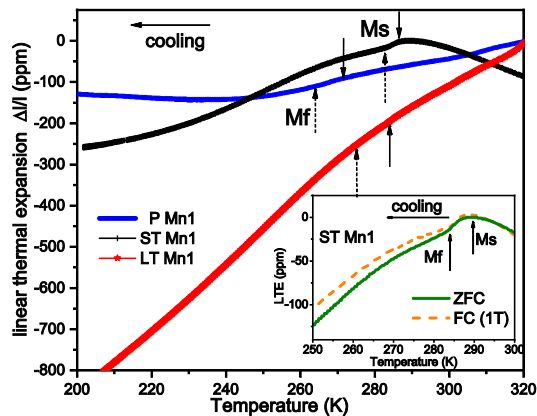


Figure.6. LTE curves during cooling (ZFC) for Mn1 samples. Inset: LTE curves during the cooling process, with (FH) and without (ZFH) magnetic field on ST Mn1.

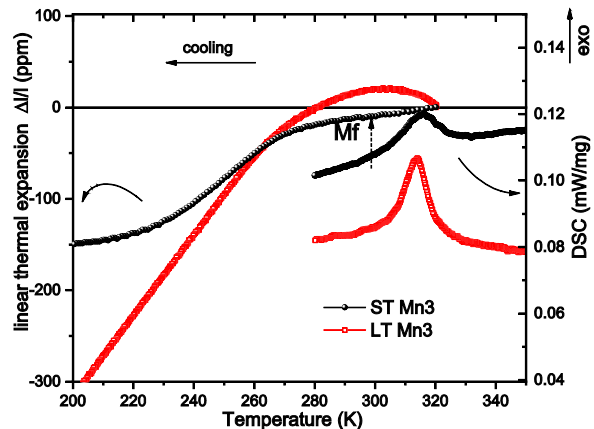


Figure.7. LTE curves during cooling (ZFC) versus DSC for ST Mn3 and LT Mn3 samples.

A recent study indicates that after annealing in $\text{Fe}_{66.8}\text{Pd}_{30.7}\text{Mn}_{2.5}$ bulk material, the dislocations and martensite variants increase their mobility. Hence, after TT, the decrease of quenched-in-defects, leads to decrease in the amount of obstacles which favour the twin boundaries movement. The LTE values at 200K provide the next comparison: $\Delta l/l_{\text{LT Mn1}} > \Delta l/l_{\text{ST Mn1}} > \Delta l/l_{\text{P Mn1}}$ (Figure.6.) and $\Delta l/l_{\text{LT Mn3}} > \Delta l/l_{\text{ST Mn3}}$ (Figure.7.). This relationship points to an increase of the active phase fraction after subsequent TT accordingly increasing the amount of the austenitic phase able to undergo MT assumption sustained by a similarity in the enthalpy values (see Inset Figure.2.). The smallest values of thermal expansion achieved in Mn3 TTs ribbons as compared to Mn1 TTs, can be a consequence of the presence of small precipitates. The LTE behaviour on cooling/heating sequences under magnetic field (1T) (Inset Figure.6.) reflects the competition between the preferential orientation under magnetic field and the spontaneous self-accommodation of martensitic variants in each grain in the polycrystalline textured samples. When applied magnetic field in austenite state, decrease the temperature and passing through MT, the martensite variants nucleate and grow along the field direction, in order to minimize the Zeeman energy. This nucleation mechanism is influence by the grain size or the existence of precipitates, cracks within the grain or at the grain boundaries [8]. The variants with the easy magnetic axis along the applied field direction grow at the expense of others, giving rise to the reduction of the contraction in the field direction. In the Inset of Figure.6., the decrease of LTE values with applied magnetic field, bellow M_f , confirms the previous report that the long axis a is the easy axis of magnetization for the martensitic state in Fe-Pd system [9].

The preliminary cell viability results (Figure.8.) generally indicate no toxicity or a tendency towards cell proliferation induced by the tested materials. However, in the case of ST Mn3 sample, significant cytotoxic effects seem to occur particularly at the highest surface (concentration) tested. Taking into account the significant increase of cell viability (i.e. cell number) for ST Mn3_S 1/2, we consider that the viability decrease corresponding to ST Mn3_S1 sample is due to density dependent inhibition of cell growth in culture rather than its cytotoxic effects.

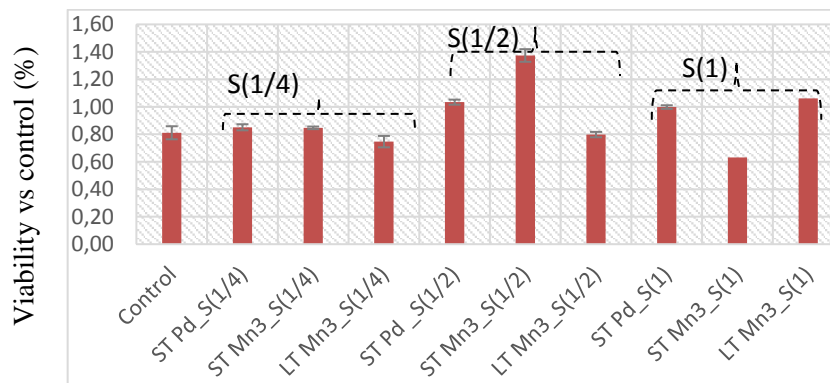


Figure.8. Cell viability for samples with different surface areas: S1 (10 mm²), S1/2 (10/2 mm²), S1/4 (10/4 mm²)

Considering the tumor nature of the used cells, it is premature to conclude whether the obtained preliminary results indicate lack of cytotoxicity or possible tumor's cells proliferation. To assess the biocompatibility of the studied materials, further complex tests on multiple, normal and tumor, cell lines are required.

4. Conclusions

The Fe₆₉Pd₃₀Mn₁ and Fe₆₇Pd₃₀Mn₃ pristine ribbons have single f.c.c. phase with high atomic disorder, without irreversible martensitic transformation, as characteristic features induced by the processing route. Subsequent TTs promote an increasing of the MT temperatures as well as changes of the transformation enthalpy. The segregation and growth of precipitates after TTs for Fe₆₇Pd₃₀Mn₃, on the account of the main transformable phase is considered to contribute essentially to the suddenly increase of the MT temperature (via the depletion of the main phase in Mn and Pd content) and the smallest values of the linear thermal expansion. The magnetoelastic behaviour reflects the competition between the preferential orientation under magnetic field and the spontaneous self-accommodation of martensitic variants in each grain in the polycrystalline textured samples and indicates that the long axis *a* of the ribbons is the easy axis of magnetization for the martensitic state. The preliminary cell viability results indicate a dependent inhibition of cell growth in culture for Fe₆₇Pd₃₀Mn₃ ribbons, rather than a cytotoxic effect.

Acknowledgment

The authors thank PhD. M. Enculescu for assistance with the SEM facility. This work was supported by Grant of Romanian Ministry of Research and Innovation, CCCDI-UEFISCDI, project number PN-III-P1-1.2-PCCDI-2017-0062/contract no.58/component project no.2, within PNCDI III.

References

- [1] Ma Y Zink M Mayr SG 2010 Appl. Phys. Lett. 96 213703.
- [2] Sofronie M Tolea F Kuncser V Valeanu M Filoti G 2015 IEEE Trans. Mag. 51 2500404.
- [3] Sánchez-Alarcos V Recarte V Pérez-Landazábal J I González MA Rodríguez- Velamazán JA 2009 Acta Materialia 57 4224.
- [4] Vokoun D Hu C T 2002 J. Alloys Compd. 346 147.
- [5] Tolea F Tolea M Sofronie M Valeanu M 2015 Solid State Communications 213 37
- [6] Oshima R 1981 Scripta Metall 15 829.
- [7] Albertini F Morellon L Algarabel P A ,M R Ibarra, LPareti, Z. Arnold, G. Calestani, 2001, J. Appl. Phys. 89 (10), 5614.
- [8] Sofronie M Tolea F Kuncser V Valeanu M 2010 J. Appl Phys. 107 113905.
- [9] Cui J Shield TW James R D 2004 Acta Mater. 52 35.